

Nonlocal QED and lepton $g-2$ anomalies

Hang Li^{1,2} and P. Wang^{1,2}

¹*Institute of High Energy Physics, Chinese Academy of Sciences, Beijing 100049, China*

²*College of Physics Sciences, University of Chinese Academy of Sciences, Beijing 100049, China*

Quantum electrodynamics is generally extended to a nonlocal QED by introducing the correlation functions. The gauge link is introduced to guarantee that the nonlocal QED is locally $U(1)$ gauge invariant. The corresponding Feynman rules as well as the proof of Ward-Takahashi identity are presented. As an example, the anomalous magnetic moments of leptons are studied in nonlocal QED. At one-loop level, besides the ordinary diagrams, there are many additional Feynman diagrams which are generated from the gauge link. It shows the nonlocal QED can provide a reasonable explanation for lepton $g-2$ anomalies.

I. INTRODUCTION

The standard model (SM) has been tested for a variety of experiments at great precision. In particular, the anomalous magnetic moment of lepton is one of the most precisely determined quantity in particle physics. The updated theoretical prediction of a_μ from standard model is $a_\mu^{\text{SM}} = 116591810(43) \times 10^{-11}$ [1]. The recent measurement of the muon anomalous magnetic moment by the E989 experiment at Fermilab shows

$$\Delta a_\mu^{\text{FNAL}} = a_\mu^{\text{FNAL}} - a_\mu^{\text{SM}} = (230 \pm 69) \times 10^{-11}, \quad (1)$$

which is a 3.3σ discrepancy from the SM prediction [2]. Combined with the previous E821 experiment at BNL [3], the result revealed a 4.2σ deviation from the prediction of the SM [2]

$$\Delta a_\mu = a_\mu^{\text{FNAL+BNL}} - a_\mu^{\text{SM}} = (251 \pm 59) \times 10^{-11}. \quad (2)$$

For electron, the theoretical prediction of a_e is $a_e^{\text{SM,B}} = 1159652182.032(720) \times 10^{-12}$ [4], where the superscript B means the fine structure constant α was measured at Berkeley with ^{137}Cs atoms [5]. The most accurate measurement of a_e has been carried out by the Harvard group and the discrepancy from SM was 2.4σ [6]

$$\Delta a_e^{\text{B}} = a_e^{\text{exp}} - a_e^{\text{SM,B}} = (-87 \pm 36) \times 10^{-14}. \quad (3)$$

However, a new determination of the fine structure constant α [7], obtained from the measurement at Laboratoire Kastler Brossel (LKB) with ^{87}Rb , improves the accuracy by a factor of 2.5 compared to the previous best measurement at Berkeley [5]. With this new α , the SM prediction for the electron magnetic moment is 1.6σ lower than the experimental data, i.e.,

$$\Delta a_e^{\text{LKB}} = a_e^{\text{exp}} - a_e^{\text{SM,LKB}} = (48 \pm 30) \times 10^{-14}. \quad (4)$$

It is interesting that the two discrepancies of Δa_e have similar size but opposite signs for still unidentified reasons [7]. The small difference of α does not affect Δa_μ because it is much larger than Δa_e . As standard model predictions almost match perfectly all other experimental information, the deviation in one of the most precisely measured quantities in particle physics provides an enduring hint for new physics.

One can compare the anomalous magnetic moments between nucleons and leptons. Since the observation of the finite size of proton by Hofstadter in 1955 [8], the electromagnetic form factors of proton and neutron have been widely studied for many decades. Theoretically, the anomalous magnetic moments of nucleon can be well described by effective field theory with the magnetic term explicitly included in the Lagrangian. However, the magnetic interaction between lepton and photon is incompatible with QED due to its non-renormalizability. Though there are some efforts to mitigate the discrepancy by correcting the theoretical calculation of the electron and muon anomalous magnetic moments in the standard model [9], many works attempt to explain the muon $g-2$ result with new physics theories beyond the standard model. For example, the standard model was extended with an additional massive gauge boson Z' which has new contributions to $(g-2)_\mu$ in Ref. [10]. New particles directly couple to muon were introduced with the new physical contributions happening at one-loop level in Ref. [11] while light millicharged particles were introduced with new contributions at two-loop level in Ref. [12] to explain the anomalies magnetic moment of muon. The authors of Ref. [13] provided a natural origin of $(g-2)_\mu$ anomaly in gauged $L_\mu-L_\tau$ model. Apart from the SM fermion content, the minimal version of this model has three heavy right handed neutrinos. In Refs. [14, 15], the authors revisited constrained low energy supersymmetry (SUSY) models to match the $(g-2)_\mu$ result. There are

also some other theories such as supergravity unified models [16], two Higgs doublet model [17, 18] and quark-lepton unification theory [19, 20], etc explaining the $(g-2)_\mu$ result. Ref. [21] is a review of new physics explanations of $(g-2)_\mu$ anomaly with up to three new fields.

Most of the above theoretical explanations focus on the $(g-2)_\mu$ anomaly and it is somewhat challenging to explain both the muon and electron $g-2$ anomalies together in the same beyond-standard-model, because of their large magnitude difference and possible opposite signs. There have been some new physical models which attempt to explain the muon and electron $g-2$ anomalies simultaneously, such as supersymmetry model [22–24], new flavor model [25], gauged $U(1)_{e-\mu}$ extension [26], two Higgs doublet model [27–30], type-III seesaw model [31], 3-3-1 model [32] and dark Z_d model [33], etc. The low-energy effective field theory and the standard model effective field theory were also applied to explain the lepton $g-2$ anomalies [34]. In addition, in Ref. [35] $SU(2)_L$ doublet and singlet vector-like heavy leptons was introduced to couple to the SM leptons via Yukawa interaction to accommodate the anomalies in the electron and muon anomalous magnetic moments. The deviations of both $(g-2)_e$ and $(g-2)_\mu$ were explained by introducing one CP-even real scalar coupled to both electron and muon with different couplings in Ref. [36]. A complex singlet scalar was introduced in Ref. [37], where the CP-odd scalar couples to electron only and the CP-even part couples to both muons and electrons. The authors of Ref. [38] considered a general framework of the scalar singlet-doublet extension of the SM scalar sector and added three sterile neutrinos so that the anomalous magnetic moments of both muon and electron can be explained by the tree-level flavor violating couplings of the light scalar to the leptons. Ref. [39] investigated all possible ways to explain both $(g-2)_e$ and $(g-2)_\mu$ with either a single scalar leptoquark or a pair of scalar leptoquarks. Since the new introduced particles have nearly no visible effects to other physical observations, they are usually related to the candidates for dark matter [40–44].

One can see that theoretical solutions to the discrepancy of lepton magnetic moments were proposed without exception by introducing new particles, symmetries and interactions beyond standard model. We tried to explain the lepton $g-2$ anomalies from another way with nonlocal QED where no new particles were introduced [45]. Nonlocal QED was inspired from nonlocal effective field theory (EFT) which reflects the non-point behavior of hadrons. The nonlocal EFT has been applied to study the nucleon electromagnetic form factors, strange form factors, parton distributions, etc [46–53]. Though QED was proved to be the fundamental theory for electromagnetic interaction, the current precise measurements on lepton anomalous magnetic moments indicate leptons could also have “structure”. Nonlocal behavior could be general for all the interactions. In our previous work, the “minimal” nonlocal extension of QED has been applied to explain the lepton $g-2$ anomalies [45]. The unique advantage of this approach is that the Lagrangian has the same gauge symmetry and same interaction as QED, except it is nonlocal. The correlation functions in the nonlocal strength tension and lepton-photon interaction make it possible to explain the discrepancies of Δa_μ and Δa_e simultaneously without introducing any new particles.

In this work, we are keen on constructing a more general nonlocal QED theory based on our previous work [45]. In Sec. II, we will introduce the general extension of the local QED Lagrangian, where both the free and interaction parts are nonlocal. The Feynman rules for the vertices including the additional interaction generated from gauge link will be presented. In Sec. III, we will prove that the Ward-Takahashi identity and charge conservation are satisfied for the nonlocal Lagrangian. All the self-energy and vertices diagrams at one-loop level will be included. The lepton anomalous magnetic moments will be studied with the nonlocal QED and numerical results will be discussed in Sec. IV. And finally Sec. V is a short summary.

II. NONLOCAL QED AND FEYNMAN RULES

The local QED Lagrangian is written as

$$\mathcal{L}^{\text{local}} = \bar{\psi}(x) (i\cancel{\partial} - m) \psi(x) - e\bar{\psi}(x)A(x)\psi(x) - \frac{1}{4}F^{\mu\nu}(x)F_{\mu\nu}(x). \quad (5)$$

Based on the same $U(1)$ symmetry, the local QED Lagrangian can be transformed into a nonlocal one using the method in [45–57]. The most general nonlocal Lagrangian can be written as

$$\begin{aligned} \mathcal{L}^{\text{nl}} = & \int d^4a \bar{\psi}\left(x + \frac{a}{2}\right) \bar{I}\left(x, x + \frac{a}{2}\right) (i\cancel{\partial} - m) \psi\left(x - \frac{a}{2}\right) I\left(x, x - \frac{a}{2}\right) F_1(a) \\ & - e \int d^4a d^4b \bar{\psi}\left(x + \frac{a}{2}\right) \bar{I}\left(x, x + \frac{a}{2}\right) A(x+b)\psi\left(x - \frac{a}{2}\right) I\left(x, x - \frac{a}{2}\right) F_1(a)F_2(a, b) \\ & - \frac{1}{4} \int d^4d F^{\mu\nu}(x)F_{\mu\nu}(x+d)F_4(d), \end{aligned} \quad (6)$$

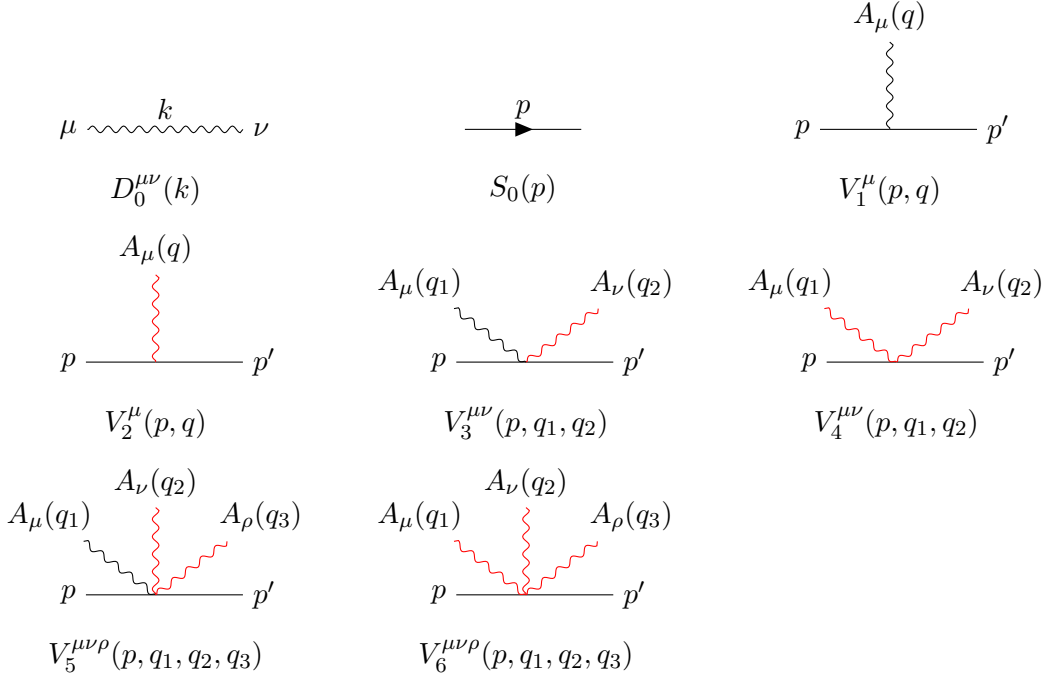


FIG. 1. Propagators and vertices in nonlocal QED appeared in one-loop diagrams. The black and red wavy lines are for photons from minimal substitution and gauge link, respectively.

where the gauge link

$$I(x, y) \equiv \exp \left(ie \int d^4c \int_x^y dz^\mu A_\mu(z+c) F_3(a, c) \right) \quad (7)$$

is introduced to guarantee the local gauge invariance. Compared with our previous work [45], here both the free Lagrangian and the interaction part are nonlocal in this general form of Eq. (6). The fermion fields ψ and $\bar{\psi}$ are located at $x - \frac{a}{2}$ and $x + \frac{a}{2}$, respectively. The photon field A_μ is located at different coordinate $x + b$. The functions $F_1(a)$, $F_2(a, b)$, $F_3(a, c)$ and $F_4(d)$ are the correlation functions normalized as

$$\int d^4a F_1(a) = \int d^4b F_2(a, b) = \int d^4c F_3(a, c) = \int d^4d F_4(d) = 1. \quad (8)$$

Certainly, \mathcal{L}^{nl} will turn back to $\mathcal{L}^{\text{local}}$ if $F_1(a) = \delta(a)$, $F_2(a, b) = \delta(b)$ and $F_4(d) = \delta(d)$. It is straightforward to prove the general nonlocal QED Lagrangian of Eq. (6) is invariant under the following gauge transformation

$$\psi(x) \rightarrow e^{i\alpha(x)}\psi(x), \quad A_\mu(x) \rightarrow A_\mu(x) - \frac{1}{e}\partial_\mu\alpha'(x), \quad (9)$$

where

$$\alpha(x) = \int d^4b \alpha'(x+b) F_2(a, b) = \int d^4c \alpha'(x+c) F_3(a, c). \quad (10)$$

With the nonlocal Lagrangian, one can derive the corresponding Feynman rules. The propagators and vertices are plotted in Fig. 1, where the black and red wavy lines in the vertices are for photons generated from the minimal substitution and gauge link, respectively. It is obvious that two or more photons can be generated from gauge link, while the minimal substitution can only generate one photon. Therefore in Fig. 1, the vertex could have one or more red photons, while it can only have one black photon at most. Since the free Lagrangian of fermion and photon fields

in Eq. (6) is nonlocal, their free propagators are modified as

$$S_0(p) = \frac{i}{\not{p} - m} \frac{1}{\tilde{F}_1(p)} \quad \text{and} \quad D_0^{\mu\nu}(k) = \frac{-ig^{\mu\nu}}{k^2} \frac{1}{\tilde{F}_4(k)}, \quad (11)$$

where $\tilde{F}_1(p)$ and $\tilde{F}_4(k)$ are Fourier transformations of the correlation functions $F_1(a)$ and $F_4(d)$, respectively. The normal fermion-photon interaction term in the nonlocal Lagrangian \mathcal{L}^{nl} generated from the minimal substitution is $\int d^4a d^4b \bar{\psi}(x + \frac{a}{2}) \not{A}(x+b) \psi(x - \frac{a}{2}) F_1(a) F_2(a, b)$. The corresponding interaction vertex is expressed as

$$V_1^\mu(p, q) = \gamma^\mu \int \frac{d^4k}{(2\pi)^4} \tilde{F}_1(k) \tilde{F}_2\left(\frac{p+p'}{2} - k, q\right) = \gamma^\mu \tilde{G}_2(p, q), \quad (12)$$

where $\tilde{G}_i(p, q)$ is defined as

$$\tilde{G}_i(p, q) \equiv \tilde{G}_i(P, q) = \int \frac{d^4k}{(2\pi)^4} \tilde{F}_1(k) \tilde{F}_i(P - k, q). \quad (13)$$

The momentum P is defined as $P \equiv \frac{p+p'}{2}$. q , p and p' are the momentum of photon, initial and final momentum of fermion, respectively.

Besides the normal interaction, the nonlocal Lagrangian \mathcal{L}^{nl} has many additional interactions where the photons are generated from the gauge link (7). The method for deducing the Feynman rules of these vertices including gauge particles has been shown in Refs. [53–56]. The related action for the interaction with one photon from the gauge link can be written as

$$S = -ie \int d^4a d^4c d^4x \bar{\psi}\left(x + \frac{a}{2}\right) G_3(a, c) (i\not{\partial}_x - m) \psi\left(x - \frac{a}{2}\right) I\left(x - \frac{a}{2}, x + \frac{a}{2}\right), \quad (14)$$

where $G_3(a, c) = F_1(a)F_3(a, c)$ and $I\left(x - \frac{a}{2}, x + \frac{a}{2}\right) = \int_{x - \frac{a}{2}}^{x + \frac{a}{2}} dz^\mu A_\mu(z + c)$. To get the Feynman rule for this vertex, we need to calculate $\int d^4a d^4c G_3(a, c) e^{iPa} I\left(x - \frac{a}{2}, x + \frac{a}{2}\right)$. Using the identity

$$\begin{aligned} \int d^4a d^4c G_3(a, c) e^{iPa} I\left(x - \frac{a}{2}, x + \frac{a}{2}\right) &= \int d^4a d^4c d^4k_1 d^4k_2 \tilde{G}_3(k_1, k_2) e^{ik_1 a} e^{ik_2 c} e^{iPa} I\left(x - \frac{a}{2}, x + \frac{a}{2}\right) \\ &= \int d^4a d^4c d^4k_1 d^4k_2 \left(\tilde{G}_3(-i\partial_a, k_2) e^{ik_1 a}\right) e^{ik_2 c} e^{iPa} I\left(x - \frac{a}{2}, x + \frac{a}{2}\right) \end{aligned} \quad (15)$$

and partial integration, it is crucial to calculate $\tilde{G}_3(-i\partial_a, k_2) e^{iPa} I\left(x - \frac{a}{2}, x + \frac{a}{2}\right)$. Following the derivation of Refs. [53–55], one can show that

$$\tilde{G}_3(-i\partial_a, k_2) e^{iPa} I\left(x - \frac{a}{2}, x + \frac{a}{2}\right) = e^{iPa} \tilde{G}_3(-iD_a, k_2) I\left(x - \frac{a}{2}, x + \frac{a}{2}\right), \quad (16)$$

where $D_a = \partial_a + iP_a$. Using the Taylor expansion and iteration method [53–56], one can finally have

$$\tilde{G}_3(-i\partial_a, k_2) I\left(x - \frac{a}{2}, x + \frac{a}{2}\right) = i \int d^4q \frac{P^\mu + q^\mu/2}{2P \cdot q + q^2} \left[\tilde{G}_3(p+q, q) - \tilde{G}_3(p, q) \right] \left[A(q) e^{iq(x+a/2)} + A(q) e^{iq(x-a/2)} \right]. \quad (17)$$

Therefore, the additional electromagnetic vertex with one photon from the gauge link is obtained as

$$V_2^\mu(p, q) = (\not{p} - m) \frac{(q + 2P)^\mu}{(q + P)^2 - P^2} \left[\tilde{G}_3(q + p, q) - \tilde{G}_3(p, q) \right]. \quad (18)$$

The additional electromagnetic vertex with two photons (one from minimal substitution with momentum q_1 and the other from the gauge link with momentum q_2) can be obtained similarly as [54–56]

$$V_3^{\mu\nu}(p, q_1, q_2) = i\gamma^\mu \frac{(q_2 + 2P)^\nu}{(q_2 + P)^2 - P^2} \left[\tilde{G}_{23}(q_2 + p, q_1, q_2) - \tilde{G}_{23}(p, q_1, q_2) \right], \quad (19)$$

where G_{ij} is defined as

$$\tilde{G}_{ij}(p, q_1, q_2) = \int \frac{d^4 k_1 d^4 k_2}{(2\pi)^8} \tilde{F}_1(k_1) \tilde{F}_i(k_2, q_1) \tilde{F}_j(P - k_1 - k_2, q_2). \quad (20)$$

The interaction vertex where two photons are both from the gauge link is expressed as

$$\begin{aligned} V_4^{\mu\nu}(p, q_1, q_2) = i(\not{p} - m) & \left\{ 2g^{\mu\nu} \frac{\tilde{G}_{33}(p + q_1 + q_2, q_1, q_2) - \tilde{G}_{33}(p, q_1, q_2)}{(P + q_1 + q_2)^2 - P^2} \right. \\ & - \frac{\tilde{G}_{33}(p + q_1 + q_2, q_1, q_2) - \tilde{G}_{33}(p, q_1, q_2)}{(P + q_1 + q_2)^2 - P^2} \left[\frac{(2P + q_1)^\mu (2P + 2q_1 + q_2)^\nu}{(P + q_1 + q_2)^2 - (P + q_1)^2} + (\mu \leftrightarrow \nu, q_1 \leftrightarrow q_2) \right] \\ & \left. + \left[\frac{[\tilde{G}_{33}(p + q_1, q_1, q_2) - \tilde{G}_{33}(p, q_1, q_2)] (2P + q_1)^\mu (2P + 2q_1 + q_2)^\nu}{((P + q_1)^2 - P^2)((P + q_1 + q_2)^2 - (P + q_1)^2)} + (\mu \leftrightarrow \nu, q_1 \leftrightarrow q_2) \right] \right\}. \quad (21) \end{aligned}$$

In the above and following equations, when $q_i \leftrightarrow q_j$, only the first argument in the function \tilde{G} makes such kind of change. There are higher order interactions with more photons generated from the expansion of the gauge link. In this manuscript, we will study the lepton anomalous magnetic moments at one-loop level. The interactions up to three photons are needed. The interaction vertex with three photons where one is from minimal substitution and the other two are from the gauge link is obtained as

$$\begin{aligned} V_5^{\mu\nu\rho}(p, q_1, q_2, q_3) = \gamma^\mu & \left\{ 2g^{\nu\rho} \frac{\tilde{G}_{233}(p + q_2 + q_3, q_1, q_2, q_3) - \tilde{G}_{233}(p, q_1, q_2, q_3)}{(P + q_2 + q_3)^2 - P^2} \right. \\ & - \frac{\tilde{G}_{233}(p + q_2 + q_3, q_1, q_2, q_3) - \tilde{G}_{233}(p, q_1, q_2, q_3)}{(P + q_2 + q_3)^2 - P^2} \left[\frac{(2P + q_2)^\nu (2P + 2q_2 + q_3)^\rho}{(P + q_2 + q_3)^2 - (P + q_2)^2} + (\nu \leftrightarrow \rho, q_2 \leftrightarrow q_3) \right] \\ & \left. + \left[\frac{[\tilde{G}_{233}(p + q_2, q_1, q_2, q_3) - \tilde{G}_{233}(p, q_1, q_2, q_3)] (2P + q_2)^\nu (2P + 2q_2 + q_3)^\rho}{((P + q_2)^2 - P^2)((P + q_2 + q_3)^2 - P^2)} + (\nu \leftrightarrow \rho, q_2 \leftrightarrow q_3) \right] \right\}, \quad (22) \end{aligned}$$

where $\tilde{G}_{ijk}(p, q_1, q_2, q_3)$ is defined as

$$\tilde{G}_{ijk}(p, q_1, q_2, q_3) = \int \frac{d^4 k_1 d^4 k_2 d^4 k_3}{(2\pi)^{12}} \tilde{F}_1(k_1) \tilde{F}_i(k_2, q_1) \tilde{F}_j(k_3, q_2) \tilde{F}_k(P - k_1 - k_2 - k_3, q_3). \quad (23)$$

The vertex for three photons which are all from the gauge link is more complicated. We can separate it into two terms as

$$V_6^{\mu\nu\rho}(p, q_1, q_2, q_3) = V_{6,a}^{\mu\nu\rho}(p, q_1, q_2, q_3) + V_{6,b}^{\mu\nu\rho}(p, q_1, q_2, q_3), \quad (24)$$

where $V_{6,a}^{\mu\nu\rho}(p, q_1, q_2, q_3)$ is proportional to $g^{\mu\nu}$ expressed as

$$\begin{aligned} V_{6,a}^{\mu\nu\rho}(p, q_1, q_2, q_3) = 2(\not{p} - m)g^{\mu\nu} & \left\{ - \frac{[\tilde{G}_{333}(p + q_1 + q_2, q_1, q_2, q_3) - \tilde{G}_{333}(p, q_1, q_2, q_3)](2P + 2q_1 + 2q_2 + q_3)^\rho}{[(P + q_1 + q_2)^2 - P^2][(P + q_1 + q_2 + q_3)^2 - (P + q_1 + q_2)^2]} \right. \\ & + \frac{\tilde{G}_{333}(p + q_1 + q_2 + q_3, q_1, q_2, q_3) - \tilde{G}_{333}(p, q_1, q_2, q_3)}{(P + q_1 + q_2 + q_3)^2 - P^2} \left[\frac{(2P + 2q_1 + 2q_2 + q_3)^\rho}{(P + q_1 + q_2 + q_3)^2 - (P + q_1 + q_2)^2} \right. \\ & \left. \left. + \frac{(2P + q_3)^\rho}{(P + q_1 + q_2 + q_3)^2 - (P + q_3)^2} \right] - \frac{[\tilde{G}_{333}(p + q_3, q_1, q_2, q_3) - \tilde{G}_{333}(p, q_1, q_2, q_3)](2P + q_3)^\rho}{[(P + q_3)^2 - P^2][(P + q_1 + q_2 + q_3)^2 - (P + q_3)^2]} \right\}. \quad (25) \end{aligned}$$

The other term $V_{6,b}^{\mu\nu\rho}(p, q_1, q_2, q_3)$ is expressed as

$$V_{6,b}^{\mu\nu\rho}(p, q_1, q_2, q_3) = (\not{p} - m) \left\{ \frac{\tilde{G}_{333}(p + q_1 + q_2 + q_3, q_1, q_2, q_3) - \tilde{G}_{333}(p, q_1, q_2, q_3)}{(P + q_1 + q_2 + q_3)^2 - P^2} \right\}$$

$$\begin{aligned}
& \times \left[\frac{(2P + 2q_2 + 2q_3 + q_1)^\mu (2P + 2q_3 + q_2)^\nu (2P + q_3)^\rho}{[(P + q_1 + q_2 + q_3)^2 - (P + q_2 + q_3)^2][(P + q_1 + q_2 + q_3)^2 - (P + q_3)^2]} + (\mu \leftrightarrow \nu, q_1 \leftrightarrow q_2) \right] \\
& - \left[\frac{\tilde{G}_{333}(p + q_2 + q_3, q_1, q_2, q_3) - \tilde{G}_{333}(p, q_1, q_2, q_3)}{(P + q_2 + q_3)^2 - P^2} \right. \\
& \times \left. \frac{(2P + 2q_2 + 2q_3 + q_1)^\mu (2P + 2q_3 + q_2)^\nu (2P + q_3)^\rho}{[(P + q_1 + q_2 + q_3)^2 - (P + q_2 + q_3)^2][(P + q_2 + q_3)^2 - (P + q_3)^2]} + (\mu \leftrightarrow \nu, q_1 \leftrightarrow q_2) \right] \\
& - \frac{\tilde{G}_{333}(p + q_3, q_1, q_2, q_3) - \tilde{G}_{333}(p, q_1, q_2, q_3)}{(P + q_3)^2 - P^2} \left[\frac{(2P + 2q_2 + 2q_3 + q_1)^\mu (2P + 2q_3 + q_2)^\nu (2P + q_3)^\rho}{[(P + q_1 + q_2 + q_3)^2 - (P + q_2 + q_3)^2][(P + q_1 + q_2 + q_3)^2 - (P + q_3)^2]} \right. \\
& \left. - \frac{(2P + 2q_2 + 2q_3 + q_1)^\mu (2P + 2q_3 + q_2)^\nu (2P + q_3)^\rho}{[(P + q_1 + q_2 + q_3)^2 - (P + q_2 + q_3)^2][(P + q_2 + q_3)^2 - (P + q_3)^2]} + (\mu \leftrightarrow \nu, q_1 \leftrightarrow q_2) \right] \\
& + (\mu \rightarrow \nu, \nu \rightarrow \rho, \rho \rightarrow \mu, q_1 \rightarrow q_2, q_2 \rightarrow q_3, q_3 \rightarrow q_1) + (\mu \rightarrow \rho, \nu \rightarrow \mu, \rho \rightarrow \nu, q_1 \rightarrow q_3, q_2 \rightarrow q_1, q_3 \rightarrow q_2) \Bigg\}. \quad (26)
\end{aligned}$$

With the above Feynman rules, one can calculate the lepton magnetic form factors with the nonlocal Lagrangian.

III. CHARGE CONSERVATION

Before we start to calculate the magnetic moments, we first show the Ward-Takahashi identity and charge conservation can be obtained with the nonlocal Lagrangian. The nonlocal Lagrangian is invariant under the local $U(1)$ transformation with the following equation

$$\int d^4x d^4a \bar{\psi} \left(x + \frac{a}{2} \right) \psi \left(x - \frac{a}{2} \right) F_1(a) \alpha(x) = \int d^4x d^4a d^4b \bar{\psi} \left(x + \frac{a}{2} \right) \psi \left(x - \frac{a}{2} \right) F_1(a) F_2(a, b) \alpha'(x + b). \quad (27)$$

Eq. (10) is obtained from the above requirement. For the fermions with momenta k_1 and k_2 , one can get the following relationship from Eq. (27) as

$$\tilde{F}_1(K) \tilde{\alpha}(k_1 - k_2) = \int d^4k_3 \tilde{F}_1(k_3) \tilde{F}_2(K - k_3, k_2 - k_1) \tilde{\alpha}'(k_1 - k_2), \quad (28)$$

where $K \equiv \frac{k_1 + k_2}{2}$. In Particular, when $k_1 = k_2$, we have

$$\tilde{F}_1(k_1) \tilde{\alpha}(0) = \int d^4k_3 \tilde{F}_1(k_3) \tilde{F}_2(k_1 - k_3, 0) \tilde{\alpha}'(0). \quad (29)$$

Meanwhile, the Fourier transformations of Eq. (8) and Eq. (10) are expressed as

$$\int d^4k \tilde{F}_2(k, 0) e^{-ik \cdot a} = 1 \quad (30)$$

and

$$\tilde{\alpha}(k) = \int d^4k' \tilde{F}_2(k', -k) \tilde{\alpha}'(k) e^{-ik' \cdot a}, \quad (31)$$

respectively. As a result, we have $\tilde{\alpha}(0) = \tilde{\alpha}'(0)$. Therefore, Eq. (29) can be rewritten as

$$\tilde{F}_1(p) = \int d^4k \tilde{F}_1(k) \tilde{F}_2(p - k, 0) \equiv G_2(p, q = 0). \quad (32)$$

In the same way, we also have

$$\tilde{F}_1(p) = \int d^4k \tilde{F}_1(k) \tilde{F}_3(p - k, 0) \equiv G_3(p, q = 0). \quad (33)$$

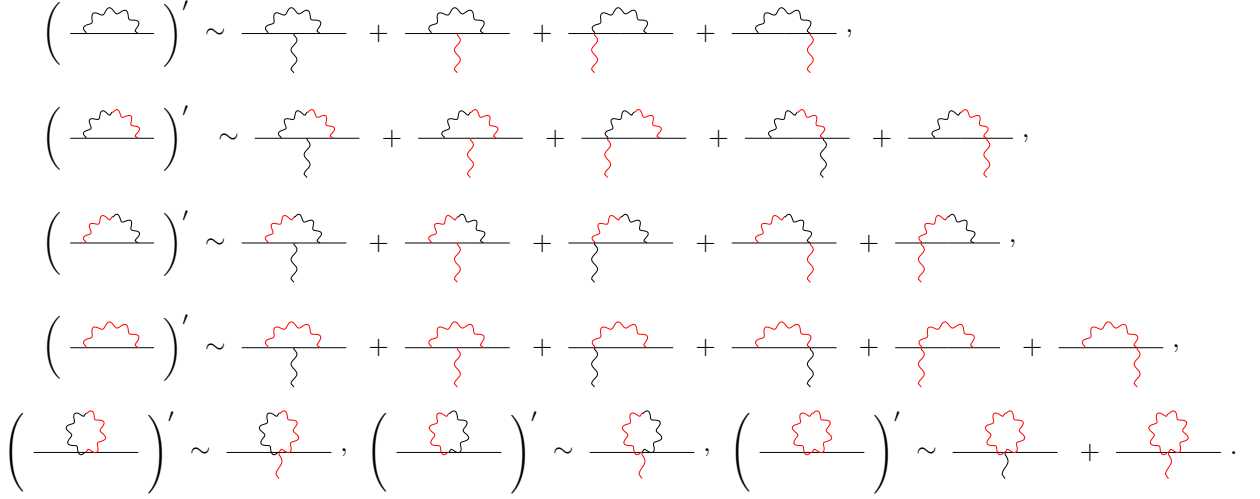


FIG. 2. Relations between lepton's self-energy diagrams and lepton-photon vertex diagrams at one-loop level in nonlocal QED. The black and red wavy lines are for photons from minimal substitution and gauge link, respectively.

With the definition of G_{ij} in Eqs. (20), one can get the relationship by using Eqs. (32) and (33) as

$$\tilde{G}_{ij}(p, q_1, q_2 = 0) = \int \frac{d^4 k_1 d^4 k_2}{(2\pi)^8} \tilde{F}_1(k_1) \tilde{F}_i(k_2, q_1) \tilde{F}_j(p - k_1 - k_2, 0) = \tilde{G}_i(p, q_1). \quad (34)$$

Similarly,

$$\tilde{G}_{ijk}(p, q_1, q_2, q_3 = 0) = \tilde{G}_{ij}(p, q_1, q_2). \quad (35)$$

Note that the above Eqs. (34) and (35) are valid for arbitrary one $q_i = 0$.

With the above equations, it is tedious but straightforward to obtain the following identities

$$\frac{dS_0(p)}{dp_\mu} = i \lim_{q \rightarrow 0} S_0(p) [V_1^\mu(p, q) + V_2^\mu(p, q)] S_0(p), \quad (36)$$

$$\frac{\partial V_1^\mu(p, q_1)}{\partial p_\nu} = i \lim_{q_2 \rightarrow 0} V_3^{\mu\nu}(p, q_1, q_2), \quad (37)$$

$$\frac{\partial V_2^\mu(p, q_1)}{\partial p_\nu} = i \lim_{q_2 \rightarrow 0} [V_3^{\nu\mu}(p, q_2, q_1) + V_4^{\mu\nu}(p, q_1, q_2)], \quad (38)$$

$$\frac{\partial V_3^{\mu\nu}(p, q_1, q_2)}{\partial p_\rho} = i \lim_{q_3 \rightarrow 0} V_5^{\mu\nu\rho}(p, q_1, q_2, q_3), \quad (39)$$

$$\frac{\partial V_4^{\mu\nu}(p, q_1, q_2)}{\partial p_\rho} = i \lim_{q_3 \rightarrow 0} [V_5^{\rho\mu\nu}(p, q_3, q_1, q_2) + V_6^{\mu\nu\rho}(p, q_1, q_2, q_3)]. \quad (40)$$

Based on the above identities, the relationship between self-energy and vertex can be established. At one-loop level, there are 7 self-energy diagrams (Fig. 5) and 24 vertex diagrams (Fig. 6) plotted in Appendix A. The total self-energy $\Sigma(p)$ and vertex $\Gamma^\mu(p, q)$ are expressed as

$$\Sigma(p) = \sum_{i=1}^7 \Sigma_i(p) \quad \text{and} \quad \Gamma^\mu(p, q) = V_1 + \sum_{i=1}^{24} \Gamma_i^\mu(p, q), \quad (41)$$

where $\Sigma_i(p)$ and $\Gamma_i^\mu(p, q)$ are all written in Appendix A. One can prove that

$$-\frac{d\Sigma_1(p)}{dp_\mu} = \lim_{q \rightarrow 0} [\Gamma_1^\mu(p, q) + \Gamma_2^\mu(p, q) + \Gamma_3^\mu(p, q) + \Gamma_5^\mu(p, q)], \quad (42)$$

$$-\frac{d\Sigma_2(p)}{dp_\mu} = \lim_{q \rightarrow 0} [\Gamma_6^\mu(p, q) + \Gamma_7^\mu(p, q) + \Gamma_8^\mu(p, q) + \Gamma_9^\mu(p, q) + \Gamma_{11}^\mu(p, q)], \quad (43)$$

$$-\frac{d\Sigma_3(p)}{dp_\mu} = \lim_{q \rightarrow 0} [\Gamma_4^\mu(p, q) + \Gamma_{12}^\mu(p, q) + \Gamma_{13}^\mu(p, q) + \Gamma_{14}^\mu(p, q) + \Gamma_{16}^\mu(p, q)], \quad (44)$$

$$-\frac{d\Sigma_4(p)}{dp_\mu} = \lim_{q \rightarrow 0} [\Gamma_{10}^\mu(p, q) + \Gamma_{15}^\mu(p, q) + \Gamma_{17}^\mu(p, q) + \Gamma_{18}^\mu(p, q) + \Gamma_{19}^\mu(p, q) + \Gamma_{20}^\mu(p, q)], \quad (45)$$

$$-\frac{d\Sigma_5(p)}{dp_\mu} = \lim_{q \rightarrow 0} \Gamma_{22}^\mu(p, q), \quad (46)$$

$$-\frac{d\Sigma_6(p)}{dp_\mu} = \lim_{q \rightarrow 0} \Gamma_{21}^\mu(p, q), \quad (47)$$

$$-\frac{d\Sigma_7(p)}{dp_\mu} = \lim_{q \rightarrow 0} [\Gamma_{23}^\mu(p, q) + \Gamma_{24}^\mu(p, q)]. \quad (48)$$

These relations can be seen clearly from Fig. 2. The derivative of the self-energy diagrams will result in the vertex diagrams. The derivative generates one external photon field which will be attached to the self-energy diagram at all possible places. For example, for the first rainbow self-energy diagram in Fig. 2, a black photon from minimal substitution or a red photon from the gauge link will be attached to the internal lepton line, while only a red photon can be attached to the vertex. For the fourth rainbow diagram, both black and red photons can be attached to the vertex.

The dressed propagator $S(p)$ can be obtained as $S(p) = S_0(p) + S_0(p)\Sigma(p)S_0(p) + S_0(p)\Sigma(p)S_0(p)\Sigma(p)S_0(p) + \dots$. With the above equations, it is straightforward to get

$$\lim_{q \rightarrow 0} S(p+q)[-i\Gamma^\mu(p+q, p)]S(p) = -\frac{dS(p)}{dp_\mu}. \quad (49)$$

This indicates the Ward–Takahashi identity

$$\lim_{q \rightarrow 0} [-iq_\mu \Gamma^\mu(p+q, p)] = \lim_{q \rightarrow 0} [S^{-1}(p+q) - S^{-1}(p)]. \quad (50)$$

The dressed propagator can be also written as

$$S(p) = \frac{iZ_2}{\not{p} - m}, \quad (51)$$

where Z_2 is the wave function renormalization constant and $Z_2 - 1 = \frac{d\Sigma(p)}{d\not{p}}|_{\not{p}=m}$. Ward–Takahashi identity of Eq. (50) implies

$$Z_2 \Gamma^\mu(p, p) = \gamma^\mu. \quad (52)$$

The Dirac and Pauli form factors are defined as [58]

$$Z_2 \Gamma^\mu(p+q, p) = \gamma^\mu F_1(q^2) + \frac{i\sigma^{\mu\nu} q_\nu}{2m} F_2(q^2). \quad (53)$$

Hence $F_1(0) = 1$. This is consistent with that the renormalized lepton charge is 1. In the next section, we will use the nonlocal QED to calculate the lepton magnetic moments to see whether the $g - 2$ anomaly can be understood.

IV. LEPTON ANOMALOUS MAGNETIC MOMENTS

By inserting the electromagnetic current into the lepton states with initial and final momenta p and p' , one can get the Dirac and Pauli form factors of lepton. The corresponding Feynman diagrams are plotted in Fig. 6 in Appendix A. With the projection method, one can obtain

$$F_1 = -\frac{A(4m^2 - q^2) - 6m^2 B}{4(4m^2 - q^2)^2}, \quad F_2 = m^2 \frac{A(4m^2 - q^2) - B(2m^2 + q^2)}{q^2(4m^2 - q^2)^2}, \quad (54)$$

where A and B are calculated from the following equations

$$A = \sum_{\text{spin}} \bar{u}(p') \Gamma_\mu u(p) \bar{u}(p) \gamma^\mu u(p') = \text{Tr} [\Gamma_\mu (\not{p} + m) \gamma^\mu (\not{p}' + m)] \quad (55)$$

and

$$B = \sum_{\text{spin}} \bar{u}(p') \Gamma_\mu u(p) \bar{u}(p) \frac{(p + p')^\mu}{m} u(p') = \text{Tr} \left[\Gamma_\mu (\not{p} + m) (\not{p}' + m) \frac{(p + p')^\mu}{m} \right]. \quad (56)$$

In this manuscript, we focus on the Pauli form factor F_2 which is related to the anomalous magnetic moment of lepton. Compared with the QED, in the nonlocal case, the one-loop vertices are much more complicated. In addition to the first diagram of Fig. 6, there are other 23 diagrams. For the first rainbow diagram, the vertex $\Gamma_1^\mu(p, q)$ is expressed as

$$\Gamma_1^\mu(p, q) = -e^2 \int \frac{d^4 k}{(2\pi)^4} V_1^\nu(p' - k, k) S_0(p - k + q) V_1^\mu(p - k, q) S_0(p - k) V_1^\rho(p, -k) D_{0\nu\rho}(k). \quad (57)$$

The corresponding Pauli form factor of vertex $\Gamma_1^\mu(p, q)$, $F_{2,1}(q^2)$ is obtained as

$$F_{2,1}(q^2) = \frac{-8ie^2 m^2}{q^2(4m^2 - q^2)^2} \int \frac{d^4 k}{(2\pi)^4} \left[\frac{(4m^2 + 2q^2)((k \cdot p)^2 + (k \cdot p')^2) - 8(m^2 - q^2)(k \cdot p)(k \cdot p')}{((p' - k)^2 - m^2)((p - k)^2 - m^2)k^2} \right. \\ \left. + \frac{(q^4 - 4m^2 q^2)(k \cdot p + k \cdot p' + k^2)}{((p' - k)^2 - m^2)((p - k)^2 - m^2)k^2} \right] \tilde{G}_2(p' - k, k) \tilde{G}_2(p - k, q) \tilde{G}_2(p, -k). \quad (58)$$

When momentum transfer $q^2 = 0$, one can get

$$F_{2,1}(0) = ie^2 \int \frac{d^4 k}{(2\pi)^4} \frac{(3k^2 + 2k \cdot p)m_l^2 - 3(k \cdot p)^2}{2k^2(k^2 - 2k \cdot p)^2 m_l^2} \tilde{G}_2(p - k, k) \tilde{G}_2(p - k, 0) \tilde{G}_2(p, -k). \quad (59)$$

For all the other diagrams, the expressions of $\Gamma_i^\mu(p, q)$ are written in Appendix A.

In the numerical calculation, we treat photon as a point particle and will not modify the photon propagator. The correlation function $F_4(a)$ in the free photon Lagrangian is chosen to be $\delta(a)$. For the lepton-photon interaction, the function $F_i(a, b)$ ($i = 2, 3$) is assumed to be factorized as $f(a)F_i(b)$ in order to simplify numerical calculation. According to Eq. (8), $f(a)$ should be an a -independent constant 1 and $\int d^4 b F_i(b) = 1$. As a result, the Fourier transformations of the correlators can be expressed as

$$\tilde{G}_i(p, q) = \tilde{F}_1(P) \tilde{F}_i(q). \quad (60)$$

For the vertex with two and three photons, they can be factorized similarly as

$$\tilde{G}_{ij}(p, q_1, q_2) = \tilde{F}_1(P) \tilde{F}_i(q_1) \tilde{F}_j(q_2), \quad (61)$$

$$\tilde{G}_{ijk}(p, q_1, q_2, q_3) = \tilde{F}_1(P) \tilde{F}_i(q_1) \tilde{F}_j(q_2) \tilde{F}_k(q_3), \quad (62)$$

where i, j and k can be 2 or 3. The subscript 2 is for photon from minimal substitution and 3 for photon from the gauge link. For the correlators in the interaction vertex, they are chosen to be

$$\tilde{F}_2(k) = \tilde{F}_3(k) = \frac{\Lambda_2^2}{\Lambda_2^2 - k^2}. \quad (63)$$

These correlators have been proposed in our earlier work on the nonlocal effective field theory and ‘‘minimal’’ version of nonlocal QED [45, 53]. The difference here is that the free Lagrangian of lepton is also nonlocal which results in a modified lepton propagator. For $\tilde{F}_1(p)$ in the free lepton propagator, it is chosen to be

$$\tilde{F}_1(p) = \frac{\Lambda_1^2 - p^2}{\Lambda_1^2}. \quad (64)$$

Since the correlator is in the denominator of the propagator, the modified propagator makes the loop integral more convergent.

In the above correlators, Λ_1 and Λ_2 are free parameters. With the parameters, the difference between nonlocal QED and standard model Δa_l^{nl} can be obtained. We determine these cutoff parameters Λ s with the experimental Δa_e and Δa_μ . We should address that nonlocal QED itself can not pre-determine the form of the correlation functions and the parameters Λ_1 and Λ_2 . They reflect the properties of the particles and should be determined by experiments. Practically, one can try and compare different correlators. The parameters Λ s will be determined to reproduce the experimental data. In this case, we determine Λ_{2e} and $\Lambda_{2\mu}$ for a given Λ_1 with the experimental Δa_e and Δa_μ for the chosen correlators.

In Fig. 3, the obtained Λ_2 versus Λ_1 are plotted. The solid, dashed and dotted lines are for muon discrepancy Δa_μ , electron discrepancies Δa_e^{LKB} and Δa_e^{B} , respectively. At each vertex, the correlator $\tilde{F}_1(k)$ makes the integral

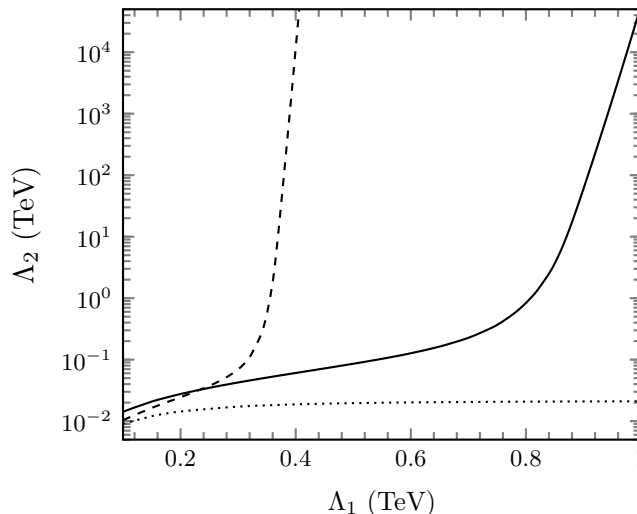


FIG. 3. The cutoff parameter Λ_2 versus Λ_1 . The solid, dashed and dotted lines are for muon discrepancy Δa_μ , electron discrepancies Δa_e^{LKB} and Δa_e^{B} , respectively.

more divergent, while $\tilde{F}_2(k)$ and $\tilde{F}_3(k)$ make the integral more convergent. For a given Λ_1 , one can always find a corresponding Λ_2 to get the experimental discrepancies. For muon, when Λ_1 is small, say less than 0.8 TeV, Λ_2 increases smoothly with the increasing Λ_1 . Meanwhile Λ_2 increases rapidly when Λ_1 is larger than about 0.8 TeV. For example, for $\Lambda_1 = 0.8$ TeV, 0.9 TeV and 1.0 TeV, the corresponding Λ_2 are 0.84 TeV, 60.23 TeV and 5.82×10^4 TeV, respectively. In order to make the nonlocal effect negligible in other electromagnetic processes, we prefer large value of Λ s (at least hundreds of GeV). For electron case, the results for the two discrepancies Δa_e^{LKB} and Δa_e^{B} are quite different. For the negative Δa_e^{B} , the obtained Λ_2^{B} is not sensitive to Λ_1 . At very broad range of Λ_1 , the value of Λ_2^{B} is around 10–20 GeV, which is too small to be reasonable. The processes, for example, the cross section $e^+e^- \rightarrow \mu^+\mu^-$ will be different from the experiments due to small cutoff parameter Λ_2 . However, for the new result of Δa_e^{LKB} , when Λ_1 is about 0.35 TeV, the obtained Λ_2^{LKB} is around 0.55 TeV. The corresponding Λ_2^{LKB} increases very quickly with the increasing Λ_1 when Λ_1 is larger than 0.35 TeV. Since for any Λ_1 , the anomalous magnetic moment of electron is infinite when Λ_2 goes to infinity, one can always get a corresponding Λ_2^{LKB} to obtain Δa_e^{LKB} for any large Λ_1 .

Therefore, the muon $g-2$ discrepancy can be well explained with large Λ s, which will not cause contradiction with the other experimental measurements. But for the electron case, Δa_e^{B} can not be reasonably reproduced in nonlocal QED. As we have pointed, the correlators in the vertex $\tilde{F}_1(k)$ and $\tilde{F}_i(k)$ $i = 2, 3$ have opposite effects. With proper choice of Λ s we can still get negative Δa_e^{nl} with large Λ s, though its absolute value is much smaller than Δa_e^{B} . For example, the calculated Δa_e^{nl} is -4.04×10^{-16} with $\Lambda_2 = 1.0$ TeV and infinite Λ_1 . Certainly, for a given Λ_1 , if Λ_2 is between Λ_2^{B} and Λ_2^{LKB} , the calculated Δa_e^{nl} is between Δa_e^{B} and Δa_e^{LKB} . For $\Lambda_1 = 1.0$ TeV, if we assume Λ_2 for electron is the same as for muon, the discrepancy Δa_e^{nl} is 8.19×10^{-14} .

To see clearly the lepton-mass dependence of the calculated discrepancy Δa_l^{nl} , in Fig. 4, we plot the Δa_l^{nl} versus lepton mass m_l with $\Lambda_1 = 1$ TeV. A small figure is plotted at the corner to show the result at small lepton mass. Because Λ_2 for electron is not well determined due to two different measurements, for any mass m_l , Λ_2 is chosen to obtain the experimental Δa_μ with $\Lambda_1 = 1$ TeV. Therefore, when $m_l = m_\mu$, Δa_l^{nl} equals to the experimental discrepancy Δa_μ . The calculated Δa_l^{nl} is bigger than Δa_e^{B} but smaller than Δa_e^{LKB} when $m_l = m_e$. The discrepancy Δa_l^{nl} increases with the increasing lepton mass and it is 5.62×10^{-7} when m_l is at the mass of τ lepton. With the nonlocal QED, both the muon and electron $g-2$ anomalies can be reasonably explained. Different from other theoretical methods, we did not introduce any new symmetries and new particles. The lepton mass dependence

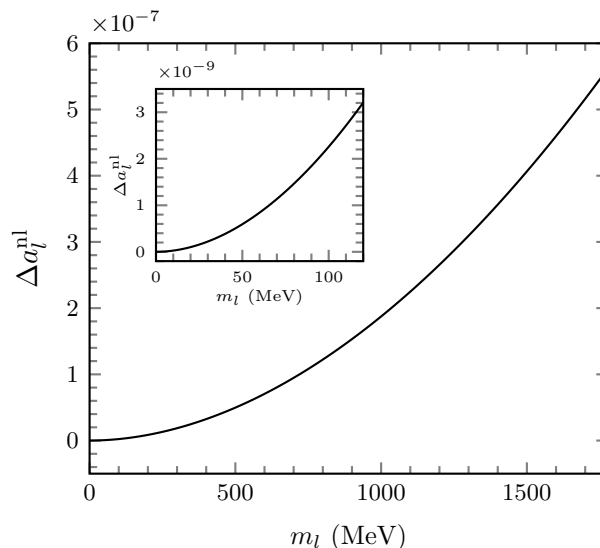


FIG. 4. The calculated discrepancy of lepton anomalous magnetic moment Δa_l^{nl} versus lepton mass m_l . Λ_1 is fixed to be 1 TeV and Λ_2 is fixed to be $\Lambda_{2\mu}$ obtained by the experimental Δa_μ with $\Lambda_1 = 1$ TeV. The small figure at the corner is for the result at small lepton mass.

of Δa_l^{nl} is naturally reproduced. It also leads to a large positive discrepancy $\Delta a_\tau^{\text{nl}}$ which can be tested by precise experiments in the future.

V. SUMMARY

In summary, we proposed a general form of nonlocal QED. With the inclusion of gauge link, the nonlocal Lagrangian is locally $U(1)$ gauge invariant. The Ward-Takahashi identity and charge conservation are also satisfied. The nonlocal Lagrangian leads to modified propagators and vertices. Besides the normal interaction from the minimal substitution, there are additional interactions generated from the gauge link. With the nonlocal QED which is one kind of extension of the standard model, we studied the anomalous magnetic moments of leptons. Both the experimental discrepancies Δa_μ and Δa_e^{LKB} can be well understood with proper choice of Λ_1 and Λ_2 in the correlators. Since the cutoff parameter Λ s should be large enough, the discrepancy Δa_e^{B} can not be reproduced, though we can still get negative Δa_e^{nl} with smaller magnitude. If the cutoff parameters are assumed to be the same for electron and muon, the calculated Δa_e^{nl} is between the two experimental values Δa_e^{B} and Δa_e^{LKB} . In addition, nonlocal QED naturally gives the lepton mass dependence of the discrepancy Δa_l^{nl} . Different from almost all the other solutions of $g - 2$ anomalies, our nonlocal QED did not introduce any new symmetries and particles.

ACKNOWLEDGMENTS

This work is supported by the NSFC under Grant No. 11975241.

Appendix A: Self energy and vertices at one-loop level

For the nonlocal QED Lagrangian there are 7 one-loop diagrams for lepton's self energy, as shown in Fig. 5. The first diagram is similar as the local QED case where the lepton-photon interaction are obtained from the minimal substitution. The expression for the first diagram is written as

$$-i\Sigma_1(p) = -e^2 \int \frac{d^4k}{(2\pi)^4} V_1^\nu(p-k, k) S_0(p-k) V_1^\mu(p, -k) D_{0\mu\nu}(k), \quad (\text{A1})$$

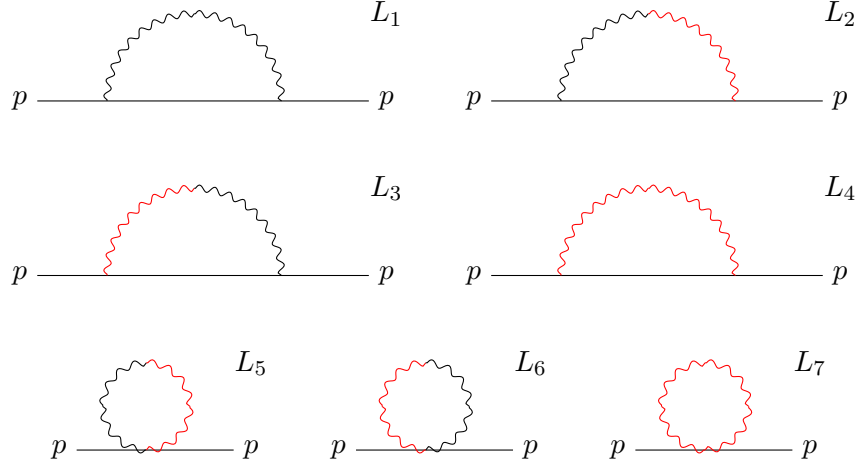


FIG. 5. Feynman diagrams of lepton self energy at one-loop level in nonlocal QED. The black and red wavy lines are for photons from minimal substitution and gauge link, respectively.

where S_0 and $D_{0\mu\nu}$ are propagators of lepton and photon. V_1^μ is the interacting vertex of Eq. (12). The diagrams of L_2 and L_3 include one photon from minimal substitution (black wavy line) and another photon from gauge link (red wavy line). The self-energy for these two diagrams are expressed as

$$-i\Sigma_2(p) = -e^2 \int \frac{d^4k}{(2\pi)^4} V_2^\nu(p-k, k) S_0(p-k) V_1^\mu(p, -k) D_{0\mu\nu}(k) \quad (\text{A2})$$

and

$$-i\Sigma_3(p) = -e^2 \int \frac{d^4k}{(2\pi)^4} V_1^\nu(p-k, k) S_0(p-k) V_2^\mu(p, -k) D_{0\mu\nu}(k), \quad (\text{A3})$$

where V_2^μ is the interacting vertex of Eq. (18). The self-energy of the rainbow diagram L_4 is expressed as

$$-i\Sigma_4(p) = -e^2 \int \frac{d^4k}{(2\pi)^4} V_2^\nu(p-k, k) S_0(p-k) V_2^\mu(p, -k) D_{0\mu\nu}(k), \quad (\text{A4})$$

where the photons in both vertices are from the gauge link. The last three are bubble diagrams, where two photons (either from minimum substitution or from gauge link) can be emitted from one vertex. The self-energy of the bubble diagram L_5 and L_6 are expressed as

$$-i\Sigma_5(p) = -e^2 \int \frac{d^4k}{(2\pi)^4} V_3^{\mu\nu}(p, -k, k) D_{0\mu\nu} \quad (\text{A5})$$

and

$$-i\Sigma_6(p) = -e^2 \int \frac{d^4k}{(2\pi)^4} V_3^{\nu\mu}(p, k, -k) D_{0\mu\nu}, \quad (\text{A6})$$

where $V_3^{\mu\nu}$ is the vertex of Eq. (19). The expression of the self-energy for the last bubble diagram L_7 is written as

$$-i\Sigma_7(p) = -e^2 \int \frac{d^4k}{(2\pi)^4} V_4^{\mu\nu}(p, k, -k) D_{0\mu\nu}, \quad (\text{A7})$$

where $V_4^{\mu\nu}$ is the vertex of Eq. (21).

All the lepton-photon vertices $\Gamma_i^\mu(p, q)$ at one-loop level are plotted in Fig. 6. The first diagram is similar as the

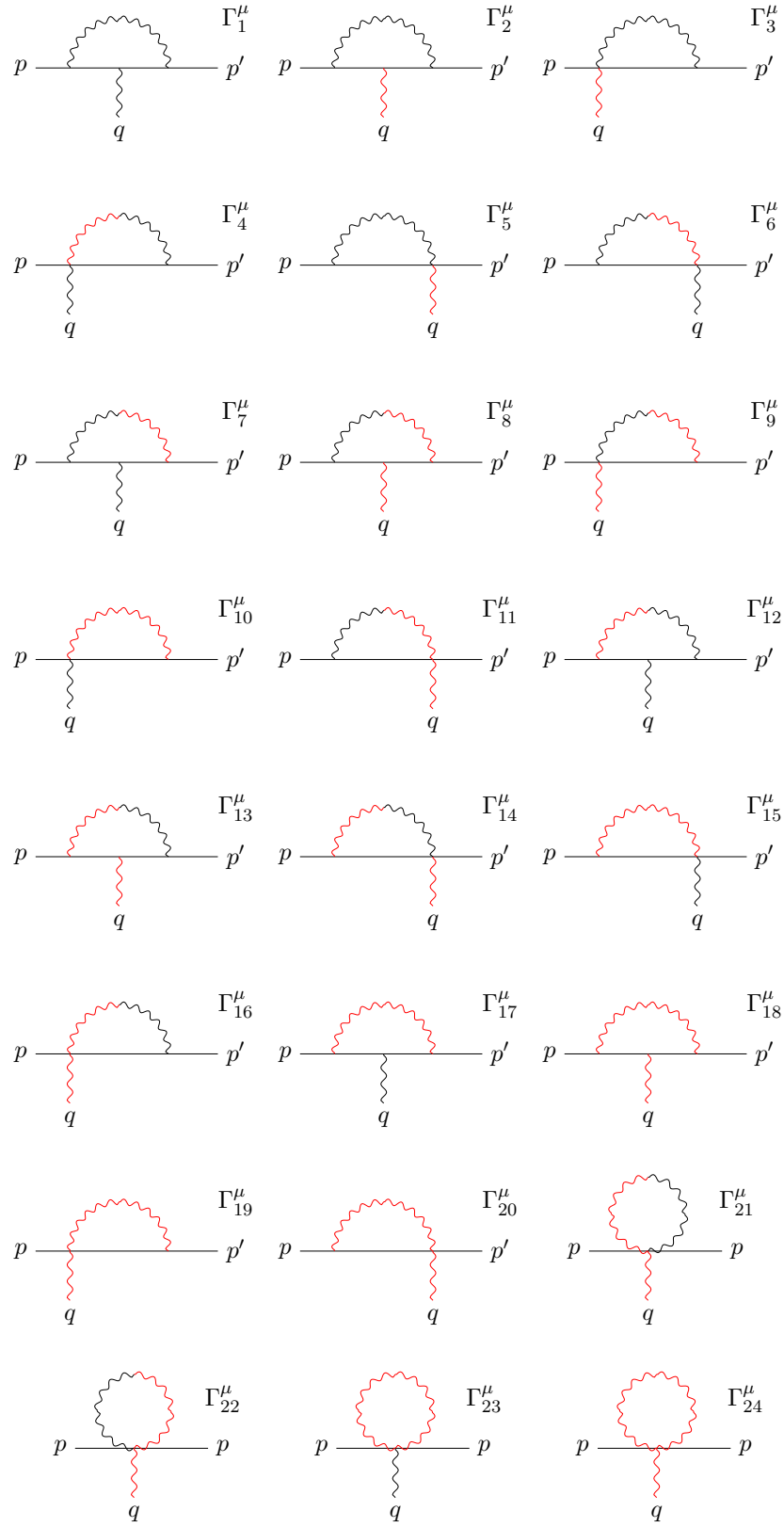


FIG. 6. Feynman diagrams for the vertices at one-loop level in nonlocal QED. The black and red wavy lines are for photons from minimal substitution and gauge link, respectively.

local QED and the expression of $\Gamma_1^\mu(p, q)$ is expressed as

$$\Gamma_1^\mu(p, q) = -e^2 \int \frac{d^4 k}{(2\pi)^4} V_1^\nu(p' - k, k) S_0(p - k + q) V_1^\mu(p - k, q) S_0(p - k) V_1^\rho(p, -k) D_{0\nu\rho}(k). \quad (\text{A8})$$

The other 23 diagrams in Fig. 6 contain additional vertices of nonlocal QED. In each diagram, both black photon (from minimal substitution) and red photon (from gauge link) can interact with lepton. At each interacting vertex, two or more photons can be emitted with only one black photon at most. The expressions of $\Gamma_i^\mu(p, q)$ for these 23 diagrams are written as

$$\begin{aligned} \Gamma_2^\mu(p, q) &= -e^2 \int \frac{d^4 k}{(2\pi)^4} V_1^\nu(p' - k, k) S_0(p - k + q) V_2^\mu(p - k, q) S_0(p - k) V_1^\rho(p, -k) D_{0\nu\rho}(k), \\ \Gamma_3^\mu(p, q) &= -e^2 \int \frac{d^4 k}{(2\pi)^4} V_1^\nu(p' - k, k) S_0(p - k + q) D_{0\nu\rho}(k) V_3^{\mu\rho}(p, -k, q), \\ \Gamma_4^\mu(p, q) &= -e^2 \int \frac{d^4 k}{(2\pi)^4} V_1^\nu(p' - k, k) S_0(p - k + q) D_{0\nu\rho}(k) V_3^{\mu\rho}(p, q, -k), \\ \Gamma_5^\mu(p, q) &= -e^2 \int \frac{d^4 k}{(2\pi)^4} V_3^{\mu\nu}(p - k, k, q) S_0(p - k) D_{0\nu\rho}(k) V_1^\rho(p, -k), \\ \Gamma_6^\mu(p, q) &= -e^2 \int \frac{d^4 k}{(2\pi)^4} V_3^{\mu\nu}(p - k, q, k) S_0(p - k) D_{0\nu\rho}(k) V_1^\rho(p, -k), \\ \Gamma_7^\mu(p, q) &= -e^2 \int \frac{d^4 k}{(2\pi)^4} V_2^\nu(p' - k, k) S_0(p - k + q) V_1^\mu(p - k, q) S_0(p - k) V_1^\rho(p, -k) D_{0\nu\rho}(k), \\ \Gamma_8^\mu(p, q) &= -e^2 \int \frac{d^4 k}{(2\pi)^4} V_2^\nu(p' - k, k) S_0(p - k + q) V_2^\mu(p - k, q) S_0(p - k) V_1^\rho(p, -k) D_{0\nu\rho}(k), \\ \Gamma_9^\mu(p, q) &= -e^2 \int \frac{d^4 k}{(2\pi)^4} V_2^\nu(p' - k, k) S_0(p - k + q) D_{0\nu\rho}(k) V_3^{\mu\rho}(p, -k, q), \\ \Gamma_{10}^\mu(p, q) &= -e^2 \int \frac{d^4 k}{(2\pi)^4} V_2^\nu(p' - k, k) S_0(p - k + q) D_{0\nu\rho}(k) V_3^{\mu\rho}(p, q, -k), \\ \Gamma_{11}^\mu(p, q) &= -e^2 \int \frac{d^4 k}{(2\pi)^4} V_4^{\mu\nu}(p - k, q, k) S_0(p - k) D_{0\nu\rho}(k) V_1^\rho(p, -k), \\ \Gamma_{12}^\mu(p, q) &= -e^2 \int \frac{d^4 k}{(2\pi)^4} V_1^\nu(p' - k, k) S_0(p - k + q) V_1^\mu(p - k, q) S_0(p - k) V_3^\rho(p, -k) D_{0\nu\rho}(k), \\ \Gamma_{13}^\mu(p, q) &= -e^2 \int \frac{d^4 k}{(2\pi)^4} V_1^\nu(p' - k, k) S_0(p - k + q) V_2^\mu(p - k, q) S_0(p - k) V_2^\rho(p, -k) D_{0\nu\rho}(k), \\ \Gamma_{14}^\mu(p, q) &= -e^2 \int \frac{d^4 k}{(2\pi)^4} V_3^{\mu\nu}(p - k, k, q) S_0(p - k) D_{0\nu\rho}(k) V_2^\rho(p, -k), \\ \Gamma_{15}^\mu(p, q) &= -e^2 \int \frac{d^4 k}{(2\pi)^4} V_3^{\mu\nu}(p - k, q, k) S_0(p - k) D_{0\nu\rho}(k) V_2^\rho(p, -k), \\ \Gamma_{16}^\mu(p, q) &= -e^2 \int \frac{d^4 k}{(2\pi)^4} V_1^\nu(p' - k, k) S_0(p - k + q) D_{0\nu\rho}(k) V_4^{\mu\rho}(p, q, -k), \\ \Gamma_{17}^\mu(p, q) &= -e^2 \int \frac{d^4 k}{(2\pi)^4} V_2^\nu(p' - k, k) S_0(p - k + q) V_2^\mu(p - k, q) S_0(p - k) V_2^\rho(p, -k) D_{0\nu\rho}(k), \\ \Gamma_{18}^\mu(p, q) &= -e^2 \int \frac{d^4 k}{(2\pi)^4} V_2^\nu(p' - k, k) S_0(p - k + q) V_2^\mu(p - k, q) S_0(p - k) V_2^\rho(p, -k) D_{0\nu\rho}(k), \\ \Gamma_{19}^\mu(p, q) &= -e^2 \int \frac{d^4 k}{(2\pi)^4} V_2^\nu(p' - k, k) S_0(p - k + q) D_{0\nu\rho}(k) V_4^{\mu\rho}(p, q, -k), \\ \Gamma_{20}^\mu(p, q) &= -e^2 \int \frac{d^4 k}{(2\pi)^4} V_4^{\mu\nu}(p - k, q, k) S_0(p - k) D_{0\nu\rho}(k) V_2^\rho(p, -k), \\ \Gamma_{21}^\mu(p, q) &= -e^2 \int \frac{d^4 k}{(2\pi)^4} V_5^{\nu\rho\mu}(p, k, -k, q) D_{0\nu\rho}, \end{aligned}$$

$$\Gamma_{22}^\mu(p, q) = -e^2 \int \frac{d^4 k}{(2\pi)^4} V_5^{\rho\nu\mu}(p, -k, k, q) D_{0\nu\rho},$$

$$\Gamma_{23}^\mu(p, q) = -e^2 \int \frac{d^4 k}{(2\pi)^4} V_5^{\mu\nu\rho}(p, q, k, -k) D_{0\nu\rho},$$

$$\Gamma_{24}^\mu(p, q) = -e^2 \int \frac{d^4 k}{(2\pi)^4} V_6^{\mu\nu\rho}(p, k, -k, q) D_{0\nu\rho},$$

where the interacting vertices $V_5^{\mu\nu\rho}$ and $V_6^{\mu\nu\rho}$ are written in Eqs. (22) and (24). With the above expressions for the self-energy and vertices, one can prove the Ward-Takahashi identity as shown in the text.

-
- [1] T. Aoyama *et al*, Phys. Rept. **887**, 1 (2020).
 - [2] B. Abi *et al*, Phys. Rev. Lett. **126**, 141801 (2021).
 - [3] G. W. Bennett *et al*, Phys. Rev. D **73**, 072003 (2006).
 - [4] T. Aoyama, T. Kinoshita, and M. Nio, Phys. Rev. D **97**, 036001 (2018).
 - [5] R. H. Parker, C. Yu, W. Zhong, B. Estey, and H. Müller, Science **360**, 191 (2018).
 - [6] D. Hanneke, S. Fogwell, and G. Gabrielse, Phys. Rev. Lett. **100**, 120801 (2008).
 - [7] L. Morel, Z. Yao, P. Cladé, and S. Guellati-Khélifa, Nature **588**, 61 (2020).
 - [8] R. Hofstadter and R. W. McAllister, Phys. Rev. **98**, 217 (1955).
 - [9] S. Borsanyi *et al*, Nature **593**, 78577, 51-55 (2021).
 - [10] P. Anastasopoulos, K. Kaneta, E. Kiritsis, and Y. Mambrini, JHEP **02**, 051 (2023).
 - [11] R. Balkin, C. Delaunay, M. Geller, E. Kajomovitz, and G. Perez, Phys. Rev. D **104**, 053009 (2021).
 - [12] Y. Bai, S. J. Lee, M. Son, and F. Ye, JHEP **11**, 019 (2021).
 - [13] D. Borah, A. Dasgupta, and D. Mahanta, Phys. Rev. D **104**, 075006 (2021).
 - [14] Z. Li, G. L. Liu, F. Wang, J. M. Yang, and Y. Zhang, JHEP **12**, 219 (2021).
 - [15] F. Wang, L. Wu, Y. Xiao, J. M. Yang, and Y. Zhang, Nucl. Phys. B **970**, 115486 (2021)
 - [16] A. Aboubrahim, P. Nath, and R. M. Syed, JHEP **06**, 002 (2021).
 - [17] A. Dey, J. Lahiri, and B. Mukhopadhyaya, Phys. Rev. D **106**, 055023 (2021).
 - [18] G. Arcadi, A. S. De Jesus, T. B. De Melo, F. S. Queiroz, and Y. S. Villamizar, Nucl. Phys. B **982**, 115882 (2022).
 - [19] P. F. Pérez, C. Murgui, and A. D. Plascencia, Phys. Rev. D **104**, 035041 (2021).
 - [20] K. Ban *et al*, PTEP **2023**, 013B01 (2023).
 - [21] P. Athron, *et al*, JHEP **09**, 080 (2021).
 - [22] M. Endo and W. Yin, JHEP **08**, 122 (2019).
 - [23] M. Badziak and K. Sakurai, JHEP **10**, 024 (2019).
 - [24] J. J. Cao, L. Meng, and Y. F. Yue, Phys. Rev. D **108**, 035043 (2023).
 - [25] L. Calibbi, M. L. López-Ibáñez, A. Melis, and O. Vives, JHEP **06**, 087 (2020).
 - [26] C. H. Chen and T. Nomura, Nucl. Phys. B **964**, 115314 (2021).
 - [27] F. J. Botella, F. Cornet-Gomez, and M. Nebot, Phys. Rev. D **102**, 035023 (2020).
 - [28] E. J. Chun and T. Mondal, JHEP **11**, 077 (2020).
 - [29] S. P. Li, X. Q. Li, Y. Y. Li, Y. D. Yang, and X. Zhang, JHEP **01**, 034 (2021).
 - [30] X. F. Han, T. J. Li, H. X. Wang, L. Wang, and Y. Zhang, Phys. Rev. D **104**, 115001 (2021).
 - [31] P. Escribano, J. Terol-Calvo, and A. Vicente, Phys. Rev. D **103**, 115018 (2021).
 - [32] T. T. Hong, N. H. T. Nha, T. P. Nguyen, L. T. T. Phuong and L. T. Hue, PTEP **2022**, 093B05 (2022).
 - [33] M. Cadeddu, N. Cargioli, F. Dordei, C. Giunti, and E. Picciau, Phys. Rev. D **104**, 011701 (2021).
 - [34] J. Aebischer *et al*, JHEP **07**, 107 (2021).
 - [35] A. Crivellin, M. Hoferichter, and P. Schmidt-Wellenburg, Phys. Rev. D **98**, 113002 (2018).
 - [36] H. Davoudiasl and W. J. Marciano, Phys. Rev. D **98**, 075011 (2018).
 - [37] J. Liu, C. E. M. Wagner, and X. P. Wang, JHEP **03**, 008 (2019).
 - [38] B. Dutta, S. Ghosh, and T. Li, Phys. Rev. D **102**, 055017 (2020).
 - [39] I. Doršner, S. Fajfer, and S. Saad, Phys. Rev. D **102**, 075007 (2020).
 - [40] B. D. Saez and K. Ghorbani, Phys. Lett. B **823**, 136750 (2021).
 - [41] P. Cox, C. Han, and T. T. Yanagida, Phys. Rev. D **98**, 055015 (2018).
 - [42] M. Chakraborti, S. Heinemeyer, and I. Saha, IFT-UAM/CSIC-23-080, 8 (2023).
 - [43] K. Ghorbani, Phys. Rev. D **104**, 115008 (2021).
 - [44] K-F. Chen, C-W. Chiang, and K. Yagyu, JHEP **09**, 119 (2020).
 - [45] Hang Li and P. Wang, J. Phys. G **50**, 115001 (2023)
 - [46] F. He and P. Wang, Chin. Phys. C **41**, 114106(2017).
 - [47] F. He and P. Wang, Phys. Rev. D **97**, 036007 (2018).

- [48] F. He and P. Wang, Phys. Rev. D **98**, 036007 (2018).
- [49] Y. Salamu, C. R. Ji, W. Melnitchouk, A. W. Thomas, and P. Wang, Phys. Rev. D **99**, 014041 (2019).
- [50] Ming-Yang Yang and P. Wang, Phys. Rev. D **102**, 056024 (2020).
- [51] F. He *et al*, Phys. Rev. D **105**, 094007 (2022).
- [52] F. He, C. R. Ji, W. Melnitchouk, A. W. Thomas, and P. Wang, Phys. Rev. D **106**, 054006 (2022).
- [53] P. Wang, F. He, C. R. Ji, and W. Melnitchouk, Prog. Part. Nucl. Phys., **129**, 104017 (2023).
- [54] J. Terning, Phys. Rev. D **44**, 887 (1991).
- [55] A. Faessler, T. Gutsche, M. A. Ivanov, Valery E. Lyubovitskij, and P. Wang, Phys. Rev. D **68**, 014011 (2003).
- [56] G. Cacciapaglia, G. Marandella, and J. Terning, JHEP **01**, 070 (2008).
- [57] P. Wang, Chin. Phys. C **35**, 223 (2011).
- [58] M. Peskin and D. Schroeder, An Introduction to Quantum Field Theory, Addison-Wesley, Reading, USA, 1995.